Solar Energy 166 (2018) 308–316

Contents lists available at ScienceDirect

Solar Energy

journal homepage: www.elsevier.com/locate/solener

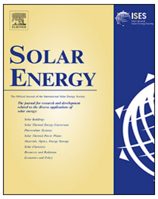

Role of Ag_3PO_4 and Fe_3O_4 on the photocatalytic performance of magnetic $Ag_3PO_4/ZnO/Fe_3O_4$ nanocomposite under visible light irradiation

Nuray Güy[a], Keziban Atacan[b], Ertuğrul Karaca[b], Mahmut Özacar[a,b,*]

[a] Sakarya University, Science & Arts Faculty, Department of Chemistry, 54187 Sakarya, Turkey
[b] Sakarya University, Biomedical, Magnetic and Semiconductor Materials Research Center (BIMAS-RC), 54187 Sakarya, Turkey

ARTICLE INFO

Keywords:
$Ag_3PO_4/ZnO/Fe_3O_4$
Microwave assisted hydrothermal synthesis
Congo red
Magnetically separable photocatalyst
Visible-light
Photodegradation mechanism

ABSTRACT

Novel magnetically separable nanocomposite photocatalyst $Ag_3PO_4/ZnO/Fe_3O_4$, prepared by the coprecipitation and microwave assisted hydrothermal synthesis, was first investigated as the photocatalyst for congo red degradation under visible light. The nano photocatalysts were systematically characterized with by X-ray diffraction (XRD), scanning electron microscopy (SEM), Fourier transform infrared spectroscopy (ATR-FTIR), vibrational sample magnetometer (VSM) measurements and UV–vis diffuse reflectance/absorbance spectroscopy (DRS). The nanocomposite $Ag_3PO_4/ZnO/Fe_3O_4$ showed enhanced photocatalytic activity compared with ZnO, ZnO/Fe_3O_4, Ag_3PO_4 and Ag_3PO_4/ZnO under the same conditions. The reasons for the highly increased activity of $Ag_3PO_4/ZnO/Fe_3O_4$ are that it allows more visible light absorption and efficient delaying the recombination of charge carriers. Also, the degradation efficiency for congo red is about 97.0% for the $Ag_3PO_4/ZnO/Fe_3O_4$ nanocomposite in the 90 min. At the end of the successful degradation process, the obtained magnetic photocatalyst was effectively separated from the suspension by applying external magnetic field.

1. Introduction

Nowadays, metal oxide semiconductor photocatalysts have become a focus of interest with their eco-friendly features in wastewater treatment and energy conversion. But, there are still some disadvantages restricting their practical applications although much effort has been devoted to preparing various photocatalysts, such as the fast recombination of photogenerated electron hole pairs and limited activity under visible light. So, it is necessary to improve highly efficient visible light driven photocatalysts for the water treatment requirements (Borges et al., 2016; Markad et al., 2017; Naseri et al., 2011; Rawal et al., 2012). ZnO is one of the most used semiconductor photocatalysts with superior properties such as surface properties, chemical stability, low cost and non-toxicity. But its wide band gap energy (E_g = 3.2 eV) restrains its use in large-scale applications in visible light (Rawal et al., 2012). Furthermore, the low rate of electron-hole separation reduces photocatalytic activity (Zhong et al., 2016). Many modified approaches for solving these problems have been investigated in the literature. One of these approaches is to shift the absorption ability of ZnO to the visible light region by compositing ZnO with a semiconductor having a narrow band gap, such as Cu_2O, Fe_2O_3, BiOI, and $ZnFe_2O_4$ (Jiang et al., 2011; Liu et al., 2013).

Silver orthophosphate (Ag_3PO_4) is a typical visible-light photocatalyst to oxidize water and photodegradation of organic pollutants by visible-light (Jiang et al., 2011; Liu et al., 2013; Rawal et al., 2012; Yi et al., 2010; Zhong et al., 2016). Besides, it has found that silver (Ag^0) nanoparticles formed on the surface of Ag_3PO_4 can retard electron-hole recombination and reduce decomposition of Ag_3PO_4. In addition, visible light absorption can be enhanced by the effect of the surface plasmon resonance of metallic silver (Dong et al., 2014; Rawal et al., 2012; Xu et al., 2014). Ag_3PO_4 has a narrow band gap energy (2.36–2.43 eV) (Rawal et al., 2012). However, studies have shown that Ag_3PO_4 always exhibits low structural stability, which prevents its common use in environmental applications. Ag_3PO_4-based photocatalysts such as AgX/Ag_3PO_4 (Bi et al., 2011), $Ag_3PO_4/In(OH)_3$ (Ren and Eckert, 2013), Ag_3PO_4/Bi_2WO_6 (Guo et al., 2013) and graphene oxide (GO)/Ag_3PO_4 (Fu et al., 2013) are designed to facilitate the separation of electron-hole pairs, light absorption, and promote the stability of the photocatalyst.

The conduction band (CB) and valence band (VB) edge potentials of Ag_3PO_4 are 0.45 eV and 2.9 eV (vs. NHE), respectively. In this case it is seen that VB potential is much lower than ZnO with +2.6 V (vs. NHE). The convenient energy band structures of Ag_3PO_4 and ZnO may lead to higher photocatalytic efficiency and structural stability. Ag_3PO_4 acts as a suitable sensitizer to enhance photocatalytic efficiency in the Ag_3PO_4/ZnO system. The role of Ag_3PO_4 is a sensitizer absorbing visible light,

---

[*] Corresponding author at: Sakarya University, Science & Arts Faculty, Department of Chemistry, 54187 Sakarya, Turkey.
E-mail address: mozacar@sakarya.edu.tr (M. Özacar).

https://doi.org/10.1016/j.solener.2018.03.045
Received 10 February 2018; Received in revised form 14 March 2018; Accepted 16 March 2018

while ZnO works as a substrate in this system (Hoseinzadeh et al., 2016; Panja et al., 2012; Shaker-Agjekandy and Habibi-Yangjeh, 2016; Singh et al., 2013). But separation of these composites from solution and recycling are difficult. The preparation of Ag_3PO_4 based photocatalysts, which are easily separated by a simple process from the suspension, remains to be a major challenge.

The recovery and reusability of the suspended ZnO-based photocatalysts by centrifugation and filtration from the reaction medium is complicated and costly. Besides, they lead to generation of secondary contamination. To overcome this problem, magnetic materials can be applied for eliminating the nanoparticles by applying external magnetic field. Without a significant reduction in the photocatalytic performance of ZnO, it can easily be recovered several times from a reaction system with a magnet (Hoseinzadeh et al., 2016; Shaker-Agjekandy and Habibi-Yangjeh, 2016; Singh et al., 2013). Due to low-cost, superior magnetic and eco-friendly features, Fe_3O_4 is one of the most commonly used magnetic materials (Fe_3O_4, γ-Fe_2O_3 and MFe_2O_4, where M is Ba^{2+}, Ni^{2+}, Co^{2+}, and Zn^{2+}) (Shekofteh-Gohari and Habibi-Yangjeh, 2015a; Yi et al., 2010). Fe_3O_4 could act as an electron-transporter and suppress the electron-hole pair recombination. So, it can be foreseen that fabrication of $Ag_3PO_4/ZnO/Fe_3O_4$ heterostructures could be combined with the advantages of activity of Ag_3PO_4/ZnO and separation due to the incorporation of Fe_3O_4 which has magnetic separation ability and conducting properties.

According to our knowledge, until now, there have been no adequate studies about the preparation of magnetic $Ag_3PO_4/ZnO/Fe_3O_4$ nanocomposite and photocatalytic efficiency even though the photocatalytic efficiencies of Ag_3PO_4. The purpose of this work is to improve a photocatalyst that exhibits excellent photocatalytic performance under visible light and is magnetically recovered. On the basis of these results, compared to ZnO and Ag_3PO_4, the as-formed $Ag_3PO_4/ZnO/Fe_3O_4$ nanocomposite was proven to demonstrate highly enhanced efficiency enhanced efficiency in photocatalytic processes and the possible photocatalytic mechanism of $Ag_3PO_4/ZnO/Fe_3O_4$ was proposed. As a result, the present work will reveal new ideas about the studies of Ag_3PO_4 based ZnO photocatalysts and produce a new photocatalyst for dye degradation. Besides, we bandy about a new idea how to utilize the complementary materials to design a novel efficient visible light driven photocatalyst.

2. Materials and methods

2.1. Materials

$FeCl_3 \cdot 6H_2O$, $FeSO_4 \cdot H_2O$, $AgNO_3$, Na_2HPO_4, $Zn(NO_3)_2 \cdot 6H_2O$, $NH_3 \cdot H_2O$, urea, $(CH_2)_6N_4$ and congo red (CR, commercial grade), were supplied from Sigma-Aldrich and used without further purification. All compounds except CR were of reagent grade.

2.2. Preparation of photocatalysts

Synthesis of ZnO: The ZnO powder was synthesized by microwave-assisted hydrothermal method. The synthesis procedure of ZnO is as follows: 0.50 g of $Zn(NO_3)_2$ was dissolved in 10 mL of distilled water then 10 mL 0.80 g of NaOH solution was dropped and stirred for 1 h to obtain a well-dissolved solution. The reaction mixture was transferred into a Teflon autoclave (100 mL) and treated at 160 °C for 5 min under temperature-controlled mode in a microwave oven (CEM Mars 5) operating at 700 W and then cooled at room temperature. The precipitate was collected centrifugation for 5 min, washed with distilled water and absolute ethanol several times. Consequently, the precipitate was dried in an oven at 60 °C for 24 h.

Synthesis of Ag_3PO_4: 5 mL of Na_2HPO_4 (0.15 M) solution was added to 100 mL of DI water, and the resulting mixture was stirred by sonication for 2 h. Afterwards, 15 mL of $AgNO_3$ solution (0.15 M) was dropped into this mixture. The obtained nanoparticles were redispersed in 100 mL of DI water and then transferred into a Teflon autoclave for hydrothermal processes at 160 °C for another 2 h (Yi et al., 2010).

Synthesis of Fe_3O_4/ZnO: Fe_3O_4/ZnO nanocomposites were fabricated in two steps with the use of simple coprecipitation and MW assisted hydrothermal synthesis. In the first step, Fe_3O_4 magnetic nanoparticles were prepared according to the method described elsewhere (Atacan and Özacar, 2015). In a 750 mL two-necked flask equipped with stirrer, 6.6725 g of $FeSO_4 \cdot H_2O$ (0.024 mol) and 11.353 g of $FeCl_3 \cdot 6H_2O$ (0.042 mol) were dissolved in 480 mL of deionized water under N_2 flow. This solution was heated at 80 °C and 200 rpm for 1 h. Then, 60 mL of ammonnia solution was added into the mixture rapidly, stirred under N_2 for another 1 h. Then the solution was cooled to room temperature. The obtained nanoparticles were separated using a permanent magnet. After decantation, magnetic nanoparticles were washed several times with deionized water and ethanol. Finally, magnetic nanoparticles were dried in a vacuum oven at 70 °C for 20 h. In the second step, 50 mg of Fe_3O_4 nanoparticles were sonicated for 5 min in 3 mmol/100 mL of $Zn(NO_3)_2 \cdot 6H_2O$ After that, 3 mmol of $(CH_2)_6N_4$ dissolved in 50 mL of water was added and obtained mixture was heated at 170 °C in a microwave oven (CEM, Mars 5) for 10 min.

Synthesis of Ag_3PO_4/Fe_3O_4/ZnO: The modified of Ag_3PO_4 nanoparticles onto the ZnO/Fe_3O_4 surface was performed by the precipitation method. Summarily, 25 mg of ZnO/Fe_3O_4 nanoparticles were dispersed in 100 mL of DI water; then 5 mL of Na_2HPO_4 (0.15 M) solution was added, and the resulting mixture was sonicated for 2 h. Afterwards, 15 mL of $AgNO_3$ solution (0.15 M) was added drop-by-drop into this mixture. The obtained nanocomposites were redispersed in 100 mL of DI water and then transferred into a Teflon autoclave for hydrothermal heating at 160 °C for another 2 h (Yi et al., 2010).

2.3. Characterization of photocatalysts

The resulting photocatalyts were confirmed by powder X-ray diffraction (XRD, Empyrean, PANalytical, The Netherlands X-ray diffractometer with Cu Kα (λ) 0.154 nm radiation) in the 2θ angles ranging from 10 to 90. The morphologies of Ag_3PO_4, Fe_3O_4/ZnO and Ag_3PO_4/Fe_3O_4/ZnO nano photocatalysts were characterized by using a scanning electron microscopy (JEOL JSM-6060 operated at 20 kV). The surface compositions of the samples were analyzed by energy dispersive spectroscopy (EDS). Magnetic measurements were carried out using vibration sample magnetometer (VSM LakeShore-7407, USA) analysis at 300 K. The UV–vis absorption spectra of the CR solution and photocatalysts were obtained by using a UV–vis spectrophotometer (UV–vis, Shimadzu UV-2600). The diffuse reflectance of the nanophotocatalysts was measured by using a UV–vis spectrophotometer fitted with a diffuse reflectance attachment. The band gap energies of the nanophotocatalysts were determined by the Kubelka–Munk function, F(R) and by extrapolating the $[F(R)h\nu]^{1/2}$versus photon energy ($h\nu$). Fourier Transform Infrared (FTIR) spectra of nanophotocatalysts were determined by using a Perkin Elmer FTIR Spectrometer (Spectrum Two) in the range 400–4000 cm^{-1} at room temperature.

2.4. Photocatalytic testing

Photocatalytic performances of obtained products were investigated by degradation of CR in water under visible light of a 128 W Xenon lamp. For each degradation processes, 50 mg of photocatalyst was dispersed in 100 mL of 16 mg/L of the CR aqueous solution. Before visible light illumination, the suspension was stirred in the dark for 30 min to achieve adsorption/desorption equilibrium of CR on the photocatalyst surface. 5 mL of the aliquots were sampled at specified time intervals, centrifuged and investigated by recording variations in the absorption band (498 nm) in the UV–vis spectra of CR. The percentage of degradation was determined by using the Eqs. (1) and (2) (Güy et al., 2016):